

Adaptation of avian influenza A (H6N1) virus from avian to human receptor-binding preference

Fei Wang^{1,2,†}, Jianxun Qi^{2,3,†}, Yuhai Bi^{2,3}, Wei Zhang^{2,3}, Min Wang^{1,2}, Baorong Zhang^{4,5}, Ming Wang¹, Jinhua Liu¹, Jinghua Yan^{2,3}, Yi Shi^{2,3,4} & George F Gao^{1,2,3,4,6,7,*}

Abstract

The receptor-binding specificity of influenza A viruses is a major determinant for the host tropism of the virus, which enables interspecies transmission. In 2013, the first human case of infection with avian influenza A (H6N1) virus was reported in Taiwan. To gather evidence concerning the epidemic potential of H6 subtype viruses, we performed comprehensive analysis of receptor-binding properties of Taiwan-isolated H6 HAs from 1972 to 2013. We propose that the receptor-binding properties of Taiwan-isolated H6 HAs have undergone three major stages: initially avian receptor-binding preference, secondarily obtaining human receptor-binding capacity, and recently human receptor-binding preference, which has been confirmed by receptor-binding assessment of three representative virus isolates. Mutagenesis work revealed that E190V and G228S substitutions are important to acquire the human receptor-binding capacity, and the P186L substitution could reduce the binding to avian receptor. Further structural analysis revealed how the P186L substitution in the receptor-binding site of HA determines the receptor-binding preference change. We conclude that the human-infecting H6N1 evolved into a human receptor preference.

Keywords crystal structure; H6N1; hemagglutinin; receptor binding

Subject Categories Microbiology, Virology & Host Pathogen Interaction

DOI 10.15252/embj.201590960 | Received 6 January 2015 | Revised 10 April 2015 | Accepted 16 April 2015 | Published online 4 May 2015

The EMBO Journal (2015) 34: 1661–1673

Introduction

Influenza A virus is an enveloped, negative-strand RNA virus with a segmented genome containing eight gene segments and that can stably adapt to humans, leading to sustained human-to-human transmission (Taubenberger & Kash, 2010; Shi *et al.*, 2014) and cause mild or severe diseases (Taubenberger & Morens, 2008). Two major proteins are

embedded on the envelope membrane of the influenza virus, hemagglutinin (HA) and neuraminidase (NA) (Gamblin & Skehel, 2010). HA binds to sialic acid receptors on target cells to initiate the virus infection, and NA cleaves the sialic acid receptor to allow virus release (Palese *et al.*, 1974; Sauter *et al.*, 1989; Liu *et al.*, 1995; Gambaryan *et al.*, 1997). Influenza A viruses are classified into distinct subtypes based on the antigenicity of their HA and NA proteins. To date, 16 functional HA subtypes (H1-H16) and nine functional NA subtypes (N1-N9) have been identified, not including recently identified HA and NA homologues (H17, H18, N10, and N11) from bat-derived influenza-like virus genomes (Li *et al.*, 2012; Tong *et al.*, 2012, 2013; Zhu *et al.*, 2012, 2013; Sun *et al.*, 2013; Wu *et al.*, 2014). The functional balance between HA and NA activities is important for viral pathogenicity, replication efficiency, and transmissibility (Baum & Paulson, 1991; Ohuchi *et al.*, 1997; Wagner *et al.*, 2000; de Wit *et al.*, 2010).

In the past century, there have been four severe influenza pandemics in 1918 (Spanish flu), 1957 (Asian flu), 1968 (Hong Kong flu), and 2009 (09-pH1N1), which were caused by H1N1, H2N2, H3N2, and again H1N1, respectively. The slightly mild 1977 Russian flu was also caused by H1N1 (Gregg *et al.*, 1978; Shenderovich *et al.*, 1979). To date, only the H1, H2, and H3 subtypes of influenza A viruses have adapted to humans, causing annual seasonal flu worldwide, in addition to the recorded pandemics mentioned above (Taubenberger & Kash, 2010). Furthermore, the H5, H7, H9, and H10 subtypes have been reported to cause sporadic infections in humans (Claas *et al.*, 1998; Yuen *et al.*, 1998; Guo *et al.*, 1999; Koopmans *et al.*, 2004; Gao *et al.*, 2013; Chen *et al.*, 2014). The seasonal flu virus preferentially binds to α 2,6-linked sialic acid receptors, whereas the avian influenza virus preferentially binds to α 2,3-linked sialic acid receptors (Imai & Kawaoka, 2012; Shi *et al.*, 2014). The receptor-binding properties of HA are a major determinant for the interspecies transmission of influenza A virus (de Graaf & Fouchier, 2014; Shi *et al.*, 2014). A relatively clear molecular understanding of the receptor-binding properties of HA has been established in limited HA subtypes, including H1, H2, H3, H5, H7, H9, H10, H13, and H16 (Eisen *et al.*, 1997; Ha *et al.*, 2001; Gamblin *et al.*, 2004; Liu

1 College of Veterinary Medicine, China Agricultural University, Beijing, China

2 CAS Key Laboratory of Pathogenic Microbiology and Immunology, Institute of Microbiology, Chinese Academy of Sciences, Beijing, China

3 Center of Influenza Research and Early-Warning, Chinese Academy of Sciences, Beijing, China

4 Research Network of Immunity and Health (RNIH), Beijing Institutes of Life Science, Chinese Academy of Sciences, Beijing, China

5 Aviation General Hospital, Beijing, China

6 National Institute for Viral Disease Control and Prevention, Chinese Center for Disease Control and Prevention (China CDC), Beijing, China

7 Office of Director-General, Chinese Center for Disease Control and Prevention (China CDC), Beijing, China

*Corresponding author. Tel: +86 10 64807688; E-mail: gaof@im.ac.cn

†These authors contributed equally to this work

et al., 2009; Lin *et al.*, 2012; Lu *et al.*, 2012, 2013a,b; Xu *et al.*, 2012, 2013; Shi *et al.*, 2013b, 2014; Xiong *et al.*, 2013a,b; Yang *et al.*, 2013; Zhang *et al.*, 2013a,b; Vachieri *et al.*, 2014), but is unknown in other HA subtypes, which represents a potential threat to human health.

The H6N1 virus has been isolated from migratory birds and domestic poultry in many countries, is considered to have low pathogenicity, and causes outbreaks in poultry with low mortality (Choi *et al.*, 2005; Lee *et al.*, 2006; Siembieda *et al.*, 2010; Corrand *et al.*, 2012; Muzyka *et al.*, 2012). Recently, a human case of infection with the H6N1 virus was reported for the first time in Taiwan in June 2013 (Wei *et al.*, 2013). Sequence analyses reveal that the human isolate (A/Taiwan/2/2013, human-H6N1) from the patient is highly homologous to the chicken H6N1 virus isolates in Taiwan (Shi *et al.*, 2013a; Wei *et al.*, 2013; Yuan *et al.*, 2013). Indeed, since 1972, infection with the H6N1 virus has been prevalent in domestic chickens in Taiwan (Lee *et al.*, 2006), and the virus circulating in Taiwan poultry has developed into a genetically unique lineage, different from the H6 subtype viruses circulating in southern China (Lee *et al.*, 2006). Recently, Wang *et al.* (2014) have assessed the receptor-binding preference, replication, and transmissibility in mammals of a series of H6 viruses isolated from live poultry markets in southern China from 2008 to 2011, pointing that H6 influenza viruses pose a potential threat to human health. However, mechanistic clues of receptor-binding determinant of H6 subtype viruses are unclear yet. An increased understanding of the molecular mechanism involved in receptor-binding properties of H6 subtype viruses could help us to predict the pandemic or epidemic potential.

Here, we performed comprehensive analysis of key residues in the receptor-binding site of Taiwan-isolated H6 HAs from 1972 to 2013. We propose that the evolution of receptor-binding properties of Taiwan-isolated H6 HAs has undergone three major processes: initially avian receptor-binding preference, secondarily obtaining human receptor-binding capacity, and recently human receptor-binding preference. This hypothesis has been confirmed by receptor-binding assessment of three representative virus isolates from these three stages, including the avian isolate (A/duck/Taiwan/0526/72, duck-H6N1) in 1972, the human-H6N1, and a homologous avian isolate (A/chicken/Taiwan/A2837/2013, chicken-H6N1). The duck-H6N1 HA preferentially binds the avian receptor, and both the chicken-H6N1 and human-H6N1 HAs bind avian and human receptor analogs, but the human-H6N1 displayed dramatically reduced binding to the avian receptor relative to the human receptor, a prerequisite for a human-adapting virus (de Graaf & Fouchier, 2014). Mutagenesis experiments have revealed that the E190V and G228S substitutions are important to obtain the human receptor-binding capacity, and further, P186L substitution is responsible for the receptor-binding preference change. Moreover, crystal structures of the human and avian HAs in complex with the receptor analogs elucidated the structural basis for the receptor-binding change.

Results

Comprehensive analysis of receptor-binding-related key residues in Taiwan-isolated H6 HAs

To obtain the mechanistic clues of receptor-binding properties of the Taiwan-isolated H6 subtype viruses, we analyzed the

Table 1. Comprehensive analysis of key residues in the receptor binding site for Taiwan-isolated H6 subtype viruses from 1972 to 2013.

| Year | No. | 186 | 190 | 226 | 228 |
|-------|-----|---------------|--------------------------|-----|-------------------|
| 1972 | 1 | P | E | Q | G |
| 1987 | 2 | P | E | Q | G |
| 1997 | 1 | P | E | Q | G |
| 1998 | 1 | P | V | Q | G |
| 1999 | 8 | P | E(2/8)/L(1/8)/ V(5/8) | Q | G |
| 2000 | 5 | P | L(2/5)/V(3/5) | Q | G(2/5)/S(3/5) |
| 2001 | 4 | P | V | Q | S |
| 2002 | 9 | P | L(2/9)/V(7/9) | Q | G(2/9)/S(7/9) |
| 2003 | 4 | P | E(1/4)/L(1/4)/ V(2/4) | Q | G(2/4)/S(2/ 4) |
| 2004 | 5 | P(4/5)/T(1/5) | E(2/5)/L(1/5)/ V(2/5) | Q | G(3/5)/S(2/5) |
| 2005 | 2 | P | V | Q | S |
| 2009 | 6 | P | V | Q | S |
| 2010 | 3 | P | V | Q | S |
| 2012 | 6 | P | V | Q | S |
| 2013 | 3 | P(2/3)/L(1/3) | V | Q | S |
| Total | 60 | | | | |

Note: The numbers in the parentheses represent the frequency.

receptor-binding-related key residues of HAs from virus isolates between 1972 and 2013. There are totally 60 H6 HA sequences from Taiwan in the GISAID (Global Initiative on Sharing All Influenza Data) database. Previous studies have been showed that amino acid substitutions at site 190, 186, 226, and 228 are important for receptor-binding change in several HA subtypes including H1, H2, H3, H5, and H7 (Shi *et al.*, 2014). Thus, we presented the residue compositions in these four sites for the 60 Taiwan-isolated H6 HA sequences (Table 1). We found that, from 1972 to 1998, the residue combination is P186/E190/Q226/G228. While from 1999 to 2004, amino acid substitutions at site 190 and 228 occurred, that the residue at site 190 could be E, L, or V and the residue at site 228 could be G or S. In 2004, a P186T substitution was also observed, but only one case in those 60 HA sequences. From 2005 to 2013, only the residue combination P186/V190/Q226/S228 was observed in the isolated H6 subtype viruses. Most recently in 2013, a P186L substitution occurred in the HA sequence of human-H6N1, compared with the highly homologous chicken-H6N1. The change of four-residue combinations can be divided into different stages, an initial stage with residue combination of P186/E190/Q226/G228, a second mutated stage with amino acid substitutions at site 190 and 228, a third stable stage with residue combination of P186/V190/Q226/S228, and a case of human infection with residue combination of L186/V190/Q226/S228.

Receptor-binding properties of duck-, chicken-, and human-derived H6N1

To evaluate the evolution process of receptor binding for the Taiwan-isolated H6 subtype viruses, we chose three representative virus

isolates with different residue combinations in the four sites (186/190/226/228) of HA, including the avian isolate (A/duck/Taiwan/0526/72, duck-H6N1) in 1972, the human-H6N1, and a homologous avian isolate (A/chicken/Taiwan/A2837/2013, chicken-H6N1). To assess the binding affinities of duck-H6N1, chicken-H6N1, and human-H6N1 to canonical avian-like and human-like receptor analogs (Jagger *et al*, 2012), we prepared soluble HA proteins and showed by surface plasmon resonance (SPR) that the duck-H6N1 HA preferentially binds to avian receptor (with an affinity of 1.17 μ M), with an undetectable binding to human receptor (Fig 1A–C). While the chicken-H6N1 and human-H6N1 HAs bind to both avian and

human receptors. The chicken-H6N1 HA still displays a binding preference for the avian receptor, with an affinity of 5.17 μ M, but low binding affinity for the human receptor (203 μ M) (Fig 1D–F). By contrast, the human-H6N1 HA displays significantly reduced binding affinity to the avian receptor (298 μ M) and a comparable binding affinity to the human receptor (268 μ M), and the binding preference for the human receptor was still evident (Fig 1G–I).

To characterize the receptor-binding properties of the avian-(duck-H6N1 and chicken-H6N1) and human-derived H6N1 (human-H6N1) at the virus level, we rescued the viruses with reverse genetics technology (Sun *et al*, 2011) and named them rDuck-H6N1,

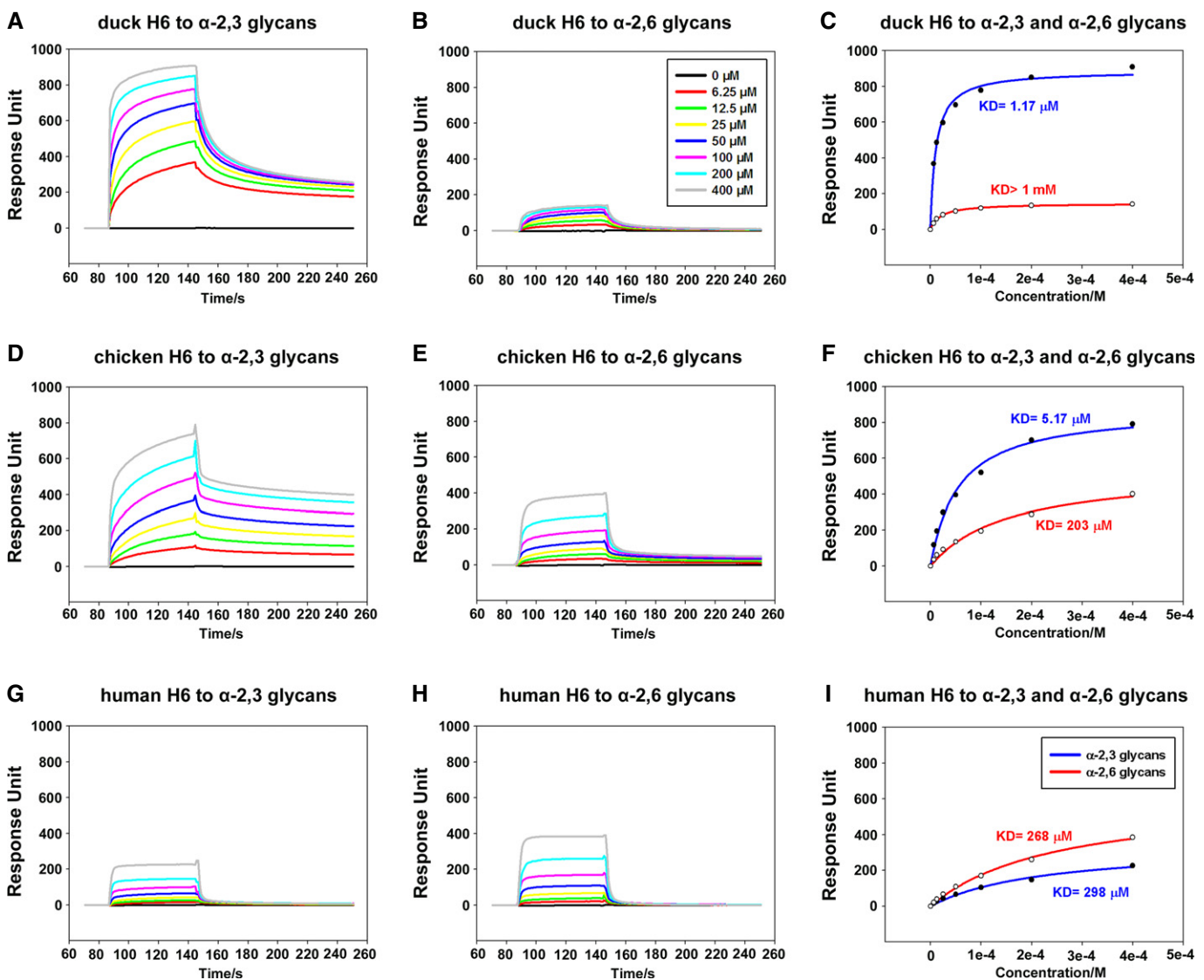


Figure 1. BIACore® binding properties of duck-H6N1, chicken-H6N1, and human-H6N1 HA proteins to either α 2,3-linked or α 2,6-linked sialylglycan receptors.

A–I BIACore® diagram of duck-H6N1 HA (A, B), chicken-H6N1 HA (D, E), and human-H6N1 HA (G, H) binding to the two receptors. Duck-H6N1 HA shows strong binding to the α 2,3-linked sialylglycan receptor but undetectable binding to the α 2,6-linked sialylglycan receptor. Chicken-H6N1 HA shows strong binding to the α 2,3-linked sialylglycan receptor but weak binding to the α 2,6-linked sialylglycan receptor. Human-H6N1 HA shows significantly reduced binding to the α 2,3-linked sialylglycan receptor and comparable weak binding to the α 2,6-linked sialylglycan receptor relative to chicken-H6N1 HA. Response units were plotted against protein concentrations (C, F and I). The K_D values were calculated by the BIACore® 3000 analysis software (BIAevaluation version 4.1). The curve of binding to α 2,3-linked sialylglycan receptor is shown in blue, and the curve of binding to α 2,6-linked sialylglycan receptor in red.

rChicken-H6N1, and rHuman-H6N1, respectively (for details, see Materials and Methods). Subsequently, we analyzed their receptor-binding properties through solid-phase binding assays using the 2009 pandemic influenza virus isolate (A/California/04/2009 (H1N1), CA04-H1N1) and avian H5N1 influenza virus isolate (A/Anhui/1/2005 (H5N1), AH05-H5N1) as control viruses that have typical human or avian receptor-binding specificity, respectively. rDuck-H6N1 preferentially bound the avian receptor, with negligible binding to human receptor (Fig 2A). rChicken-H6N1 bound both the human and avian receptors, as did rHuman-H6N1, though with reduced binding to the avian receptor (Fig 2B and C). As a control, CA04-H1N1 specifically bound the human receptor (Fig 2D) and AH05-H5N1 specifically bound the avian receptor (Fig 2E).

Mutagenesis work on chicken-H6N1 HA

To confirm the residues at four positions 186–190–226–228 are receptor-binding determinants of H6 subtype HAs, we investigated the effect of amino acid substitutions at these four positions in the same chicken-H6N1 HA background. We found that the chicken-H6-190E-228G mutant mimics the binding mode of duck-H6N1 HA, which preferentially binds to avian receptor (Fig 3A–C), and both the mutant and duck-H6N1 HA share the residue combination P186/E190/Q226/G228. Then, the chicken-H6-186L mutant mimics

the binding mode of human-H6N1 HA, which displays a dramatically reduced binding to avian receptor and preferential binding to human receptor (Fig 3D–F), and both of the mutant and human-H6N1 HA share the residue combination L186/V190/Q226/S228. In a word, the mutagenesis work on chicken-H6N1 HA reveals that the E190V and G228S substitutions are determinants to confer the H6 HA with human receptor-binding capacity, and the P186L substitution can dramatically reduce the binding to avian receptor.

Structures of chicken- and human-H6N1 HAs in complex with receptor analogs

To elucidate the structural basis of receptor binding for chicken-H6N1 HA (cH6) and human-H6N1 HA (hH6), we used X-ray crystallography to determine the structures of cH6 and hH6, both in free form and in complex with two sialo-pentasaccharides: 3'SLNLN and 6'SLNLN. These sialo-pentasaccharides are analogs of the avian and human receptors, respectively, containing the three terminal saccharides (Sia-Gal-GlcNAc). Both cH6 and hH6 display a typical homotrimer oligomerization as seen in other HA subtypes and exhibit a cleaved HA1/HA2 form.

The structure of cH6 with the avian receptor analog 3'SLNLN reveals that the ligand binds in a *cis* conformation (Fig 4A), unlike what is seen in all other previously reported avian HA/avian

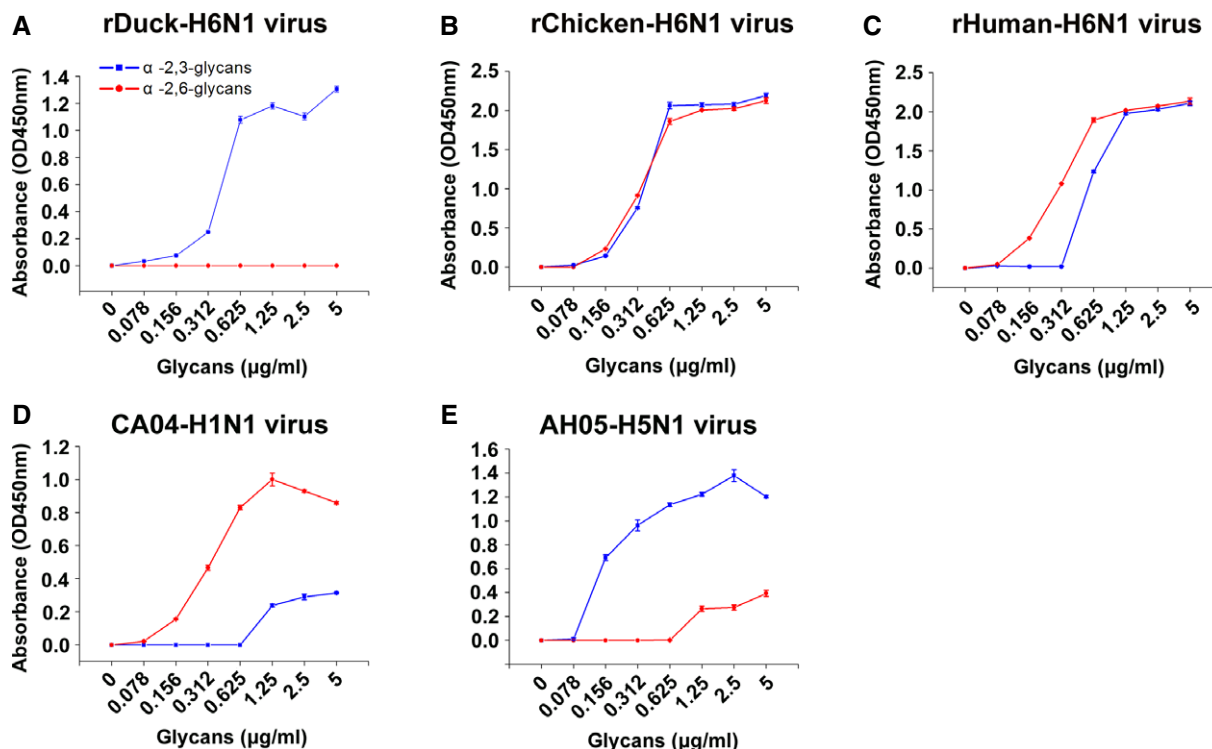
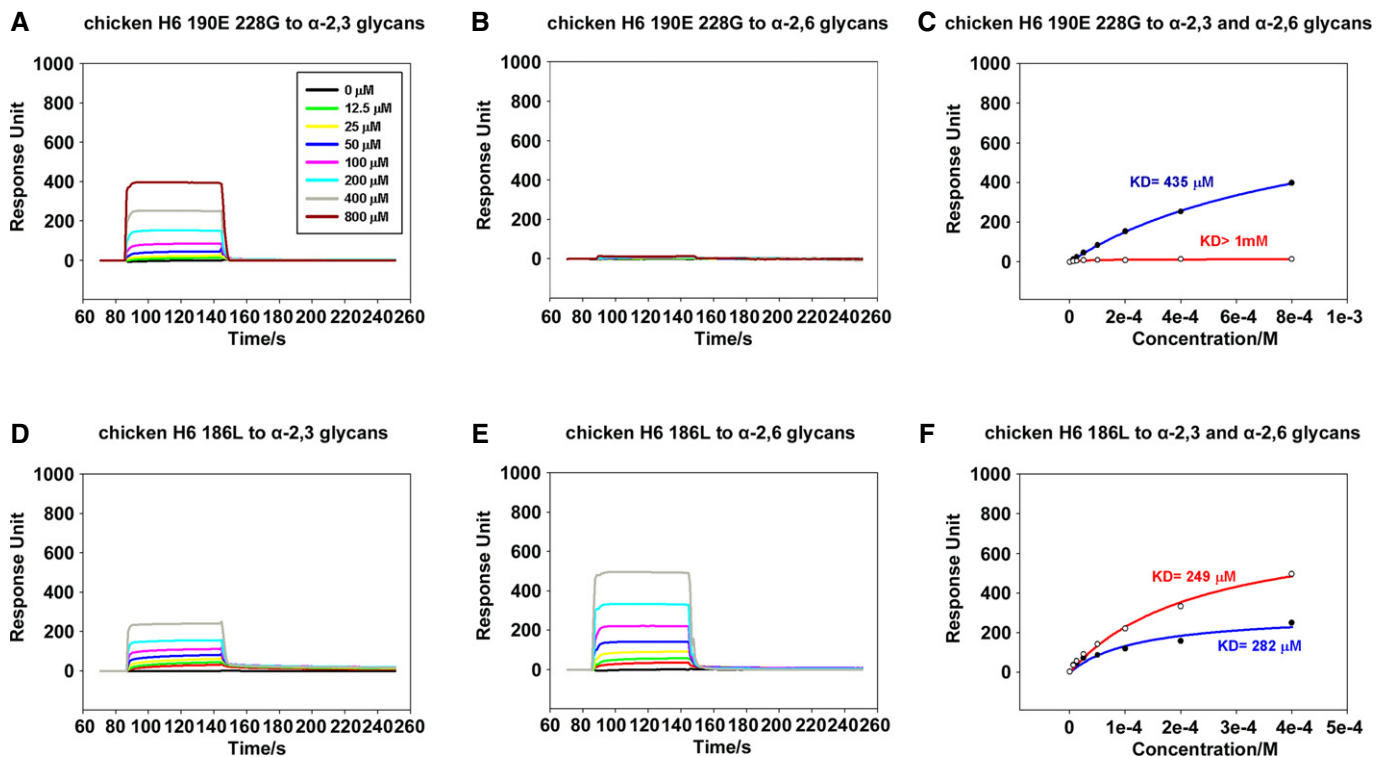


Figure 2. Receptor-binding properties at the virus level.

A–E Solid-phase binding assay for (A) rDuck-H6N1 (reverse genetics rescued A/duck/Taiwan/0526/72), (B) rChicken-H6N1 (reverse genetics rescued A/chicken/Taiwan/A2837/2013), (C) rHuman-H6N1 (reverse genetics rescued A/Taiwan/2/2013), (D) CA04-H1N1 (A/California/04/2009), and (E) AH05-H5N1 (A/Anhui/1/2005) viruses to both α 2,3-linked (3'SLNLN) and α 2,6-linked sialylglycan receptors (6'SLNLN). Binding to 3'SLNLN is colored in blue and 6'SLNLN in red. rDuck-H6N1 preferentially binds to 3'SLNLN, with no detectable binding to 6'SLNLN. rChicken-H6N1 binds both 3'SLNLN and 6'SLNLN, while rHuman-H6N1 preferentially binds to 6'SLNLN. As controls, CA04-H1N1 specifically binds to 6'SLNLN and AH05-H5N1 specifically binds to 3'SLNLN were used. Error bars represent SD of the mean, which is calculated from three independent repeats.

**Figure 3. Mutagenesis experiments on chicken-H6N1 HA.**

A–F BIACore® diagram of chicken-H6N1-190E-228G HA mutant (A, B) and chicken-H6N1-186L HA mutant (D, E) binding to the two receptors. The chicken-H6N1-190E-228G HA mutant shows preferential binding to the α 2,3-linked sialylglycan receptor but undetectable binding to the α 2,6-linked sialylglycan receptor, which mimics the duck-H6N1 HA. The chicken-H6N1-186L HA mutant shows significantly reduced binding to the α 2,3-linked sialylglycan receptor and weak binding to the α 2,6-linked sialylglycan receptor, which mimics human-H6N1 HA. Response units were plotted against protein concentrations (C, F). The K_D values were calculated by the BIACore® 3000 analysis software (BIAsolution version 4.1). The curve of binding to α 2,3-linked sialylglycan receptor is shown in blue, and the curve of binding to α 2,6-linked sialylglycan receptor is shown in red.

receptor analog complexes. The ‘avian-signature’ residue Q226 forms two hydrogen bonds with the Sia-1, and the residue S228 forms one hydrogen bond with the Sia-1. Interestingly, N137 forms two hydrogen bonds with the Gal-2, which has not been observed in other naturally occurring HA/receptor complexes. Usually, the residues of the 130-loop only form hydrogen bonds with the Sia-1, aside from one example, that is, that of the airborne-transmissible H5 mutant bound to the avian receptor (Zhang *et al.* 2013a). By contrast, the structure of cH6 with the human receptor analog 6'SLNLN reveals that the ligand binds in a *trans* conformation (Fig 4B). Similarly, the ‘avian-signature’ residue Q226 forms two hydrogen bonds with the

Sia-1, and S228 forms one hydrogen bond with the Sia-1. However, N137 forms only one hydrogen bond with the Gal-2.

The structure of hH6 with the avian receptor analog 3'SLNLN reveals that the ligand binds in a *cis* conformation (Fig 4C), similar to that seen in the cH6/avian receptor complex described above. The ‘avian-signature’ residue Q226 forms two hydrogen bonds with the Sia-1, and S228 forms one hydrogen bond with the Sia-1. In this case, N137 does not form any hydrogen bonds with the Gal-2 but forms one hydrogen bond with the Sia-1. The structure of hH6 with the human receptor analog 6'SLNLN shows that the ligand binds in a *trans* conformation (Fig 4D), similar to that seen in the cH6/human

Figure 4. Molecular interactions of cH6 and hH6 with either avian or human receptor analogs.

The three secondary structural elements of the binding site (i.e., the 130-loop, 190-helix, and 220-loop) are labeled in ribbon representation, together with selected residues in stick representation. The hydrogen bonds are shown as dashed lines. The Sia-1 moiety of the receptor analogs is colored in red, the Gal-2 moiety is colored in blue, and the GlcNAc-3 moiety is colored in yellow.

- A, B cH6 with the avian receptor analog 3'SLNLN (α 2,3) pentasaccharide (A) or human receptor analog 6'SLNLN (α 2,6) pentasaccharide (B) bound. The 3'SLNLN binds in a *cis* conformation, and the 6'SLNLN binds in a *trans* conformation.
- C, D hH6 with the avian receptor analog 3'SLNLN (C) or the human receptor analog 6'SLNLN (D) bound. The 3'SLNLN binds in a *cis* conformation, and the 6'SLNLN binds in a *trans* conformation.
- E The detailed differences in the interaction with the avian receptor analog are shown via comparisons between cH6/3'SLNLN and hH6/3'SLNLN complexes. The residues at position 186 exhibit different effects on the overall conformations of the receptor analog, due to different lengths of the side chains of the residues. In the cH6/3'SLNLN complex, N137 forms two hydrogen bonds with the avian receptor analog, ensuring strong binding. In the hH6/3'SLNLN complex, the hydrogen bonds between N137 and receptor analog are destroyed, resulting in reduced binding.
- F In the cH6/6'SLNLN complex, N137 forms a hydrogen bond with the Gal-2. In the hH6/6'SLNLN complex, Q226 forms a hydrogen bond with the Gal-2. The Gal-2 rotates by \sim 60°, which might result from the P186L substitution.

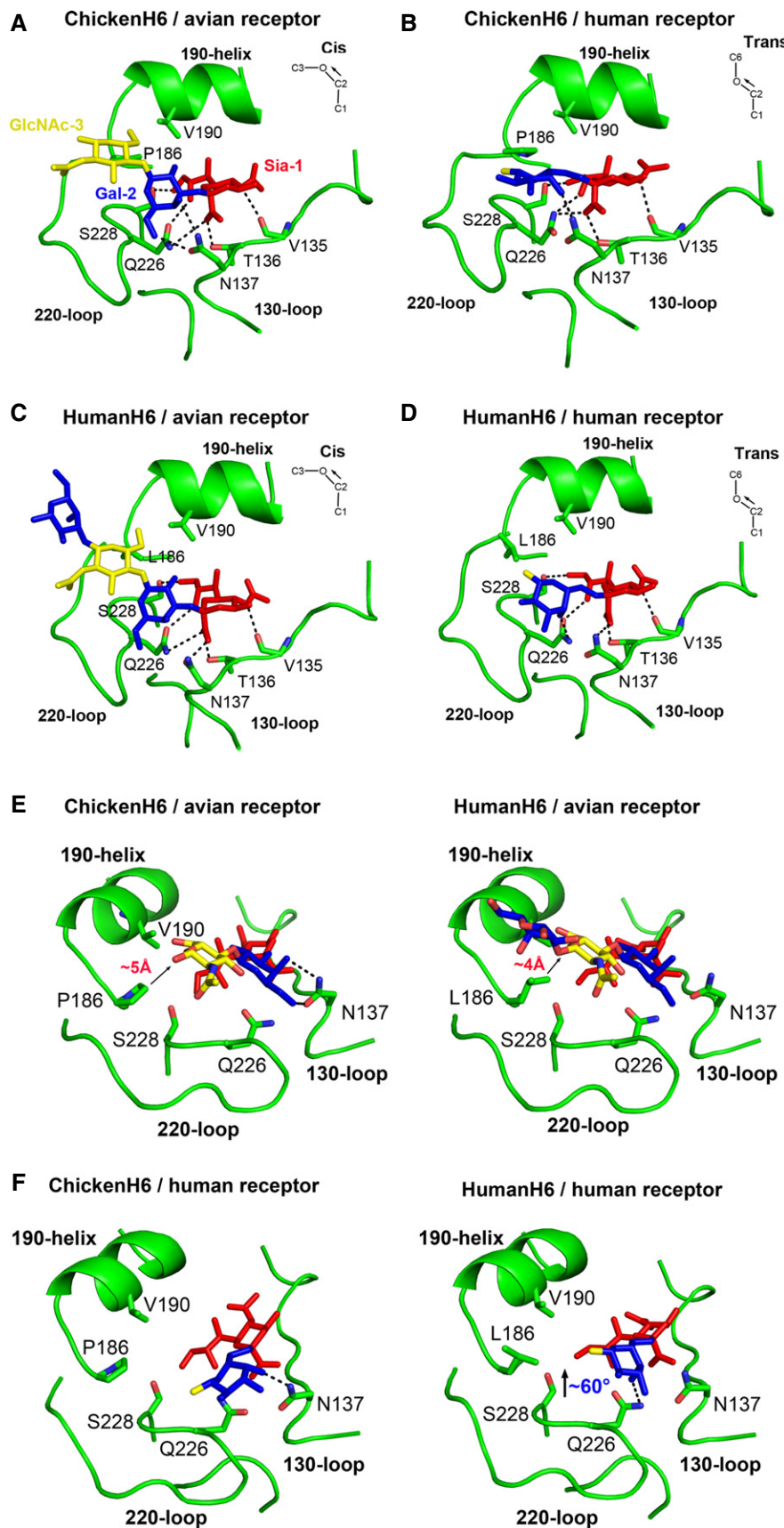


Figure 4.

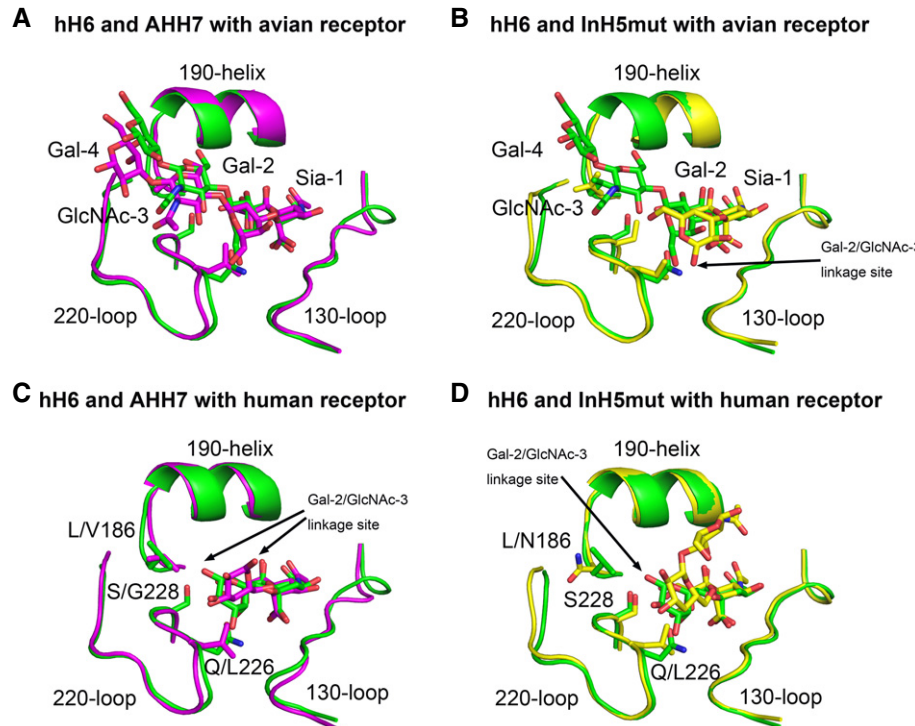


Figure 5. Comparison of the complex structures of hH6, human-infecting H7, and transmissible H5 bound to the avian or human receptor analog.

The HAs from the human-infecting H7N9 isolate (Anhui/1/2013, AHH7) and transmissible H5N1 isolate (mutant form of A/Indonesia/5/2005, InH5mut) were chosen to compare.

A, B Comparison of hH6, AHH7, and InH5mut complexes with avian receptor analogs. The avian receptor analogs bind in a similar *cis* conformation in both the hH6 and AHH7 complexes. Despite the avian receptor analog adopting a similar *cis* conformation in the InH5mut complex, the Gal-2 moiety rotates by ~180°, pointing the Gal-2/GlcNAc-3 linkage site away from the receptor-binding site.

C, D Comparison of hH6, AHH7, and InH5mut complexes with human receptor analogs. The human receptor analog binds in a *trans* conformation in the hH6 complex, and the Gal-2/GlcNAc-3 linkage site points toward the space between the 220-loop and 190-helix. In contrast, the human receptor analogs bind in a similar *cis* conformation in the AHH7 and InH5mut complexes, but the directions of the Gal-2/GlcNAc-3 linkage site are different. The Gal-2/GlcNAc-3 moieties fold back and go through the 190-helix in the InH5mut complex, like that in the pandemic H1, H2, and H3 complexes, while the Gal-2/GlcNAc-3 linkage points out from the receptor-binding site in the AHH7 complex.

receptor complex described above. The ‘avian-signature’ residue Q226 forms one hydrogen bond with the Sia-1 and one hydrogen bond with the Gal-2, and S228 forms one hydrogen bond with the Sia-1. Similarly, N137 forms one hydrogen bond with the Sia-1.

Structural basis of the receptor-binding preference change

Further structural analysis indicated that a subtle conformation adjustment occurs when cH6 and hH6 bind to different receptor analogs, as a result of the P186L substitution. The structures show that in cH6 bound to 3'SLNLN, the distance between P186 and the GlcNAc-3 is ~5 Å, without any van der Waals (vdw) interactions (Fig 4E). However, when hH6 is bound to 3'SLNLN, the distance between L186 and the GlcNAc-3 is ~4 Å due to the long side chain of L186 (Fig 4E). L186 creates a more hydrophobic environment for the GlcNAc-3 and affects the overall conformation of the ligand through vdw interactions. Thus, the hydrogen bonds between N137 and the Gal-2 are missing in structure of hH6 bound to 3'SLNLN compared to that in cH6 bound to the ligand. This lack of hydrogen bonds may result in the slightly reduced binding of the avian receptor analog by hH6.

In contrast, when both cH6 and hH6 bind to the human receptor analog 6'SLNLN, the ligands adopt a similar *trans* conformation. However, there is a ~60° difference in rotation around the Gal-2 C5-C6 bond between the cH6 and hH6 complexes (Fig 4F). As a result of this rotation, the Gal-2 forms a hydrogen bond with the N137 in the cH6 complex (Fig 4F), while in the hH6 complex, the Gal-2 forms a hydrogen bond with Q226 (Fig 4F). This rotation may result from the P186L substitution, as we cannot observe the remaining moieties of the ligand in the cH6 and hH6 complexes due to possible flexible binding.

Comparison with other HA subtypes

To explore the pandemic potential of the human-derived avian influenza A H6N1 virus from the basis of structural features, we compared the hH6 complex structures with those from the recent human-infecting avian influenza A H7N9 virus and a transmissible H5N1 virus. For comparison, we chose the HA complex structures from the H7N9 virus isolate (A/Anhui/2013/1, AHH7) and the transmissible H5N1 mutant virus isolate (mutant form of A/Indonesia/5/2005, InH5mut).

When bound to the avian receptor, hH6 binds the ligand in a *cis* conformation similar to that of AHH7, but the glycan moieties sit lower in the AHH7 complex structure than in the hH6 complex structure (Fig 5A). In contrast, despite the fact that the avian ligand adopts a *cis* conformation in the InH5mut complex, the Gal-2 moiety is rotated by ~180°, pointing the Gal-2/GlcNAc-3 linkage site out from the receptor-binding site (Fig 5B). This discrepancy may result from the different residues at position 186. Hydrophobic residues (L186 and V186) are observed for hH6 and AHH7, but a hydrophilic residue (N186) is found in InH5mut.

When bound to the human receptor, hH6 binds the ligand in a *trans* conformation, and the Gal-2/GlcNAc-3 linkage site points toward the space between the 220-loop and 190-helix (Fig 5C). In contrast, AHH7 and InH5mut bind the ligand in a similar *cis* conformation, but the directions of the Gal-2/GlcNAc-3 linkage site are different. The Gal-2/GlcNAc-3 moieties fold back and go through the 190-helix in the InH5mut complex, as in the pandemic H1, H2, and H3 complexes, while the Gal-2/GlcNAc-3 linkage points out from the receptor-binding site in the AHH7 complex (Fig 5C and D).

Discussion

During the adaption of influenza A virus to humans, the receptor-binding properties of the HA protein play a major role in interspecies transmission (Shi *et al.*, 2014). To date, only the H1, H2, and H3 subtypes of influenza virus have naturally adapted to humans, causing seasonal flu or occasional pandemics (Taubenberger & Kash, 2010). Other HA subtypes are yet circulating in avian species, and some of them can cause sporadic human infections, such as H5, H7, H9, H10, and recently H6 (Claas *et al.*, 1998; Yuen *et al.*, 1998; Guo *et al.*, 1999; Koopmans *et al.*, 2004; Gao *et al.*, 2013; Wei *et al.*, 2013; Chen *et al.*, 2014). Prior to the ‘host jump’, the receptor-binding properties must change from an avian receptor preference to human receptor preference via amino acid substitutions in the receptor-binding site of HA. Understanding of the molecular mechanisms of receptor-binding shifts is important to pre-warn against and control influenza virus infections, including possible future pandemics or epidemics.

For different HA subtypes, the molecular mechanisms of receptor-binding shifts are distinct (Shi *et al.*, 2014). For H1 subtype, it is known that the shift in receptor-binding specificity is achieved by two amino acid substitutions (E190D and G225D, amino acids in H3 numbering) in the receptor-binding site (Gamblin *et al.*, 2004; Xu *et al.*, 2012; Zhang *et al.*, 2013b), while for the H2 and H3 subtypes, Q226L and G228S substitutions occur in the receptor-binding site (Connor *et al.*, 1994; Eisen *et al.*, 1997; Liu *et al.*, 2009). For the H5 subtype, the Q226L substitution and loss of glycosylation in the 150-loop of the receptor-binding site are enough to change the receptor-binding preference (Herfst *et al.*, 2012; Imai *et al.*, 2012; Lu *et al.*, 2013b; Xiong *et al.*, 2013a; Zhang *et al.*, 2013a). In contrast, for H7 subtype, the human receptor-binding capacity can be achieved by several substitutions from hydrophilic residues to hydrophobic residues, including S138A, G186V, T221P, and Q226L (Shi *et al.*, 2013b; Xiong *et al.*, 2013b; Xu *et al.*, 2013; Yang *et al.*, 2013). To date, the H7 subtype retains strong avian receptor-binding capacity, which is a restraining factor for efficient human-to-human transmission.

In the case of the H6 subtype reported here, the E190V and G228S substitutions are important for the human receptor-binding capacity,

and the P186L substitution is important for the receptor-binding preference shift by reducing avian receptor binding. It is noted that the chicken-H6N1-190E-228G HA mutant does not have strong binding affinity as the duck-H6N1 HA does (Fig 3), indicating other amino acid substitutions in the receptor-binding site could alter the binding affinity to avian receptor. The structural analysis revealed that the more bulky Leu residue creates a more hydrophobic environment for the GlcNAc-3 of the avian receptor analog and affects the overall conformation of the ligand via van der Waals interactions. Thus, this conformational adjustment destroys the hydrogen bonds between N137 and the Gal-2, resulting in weaker avian receptor binding. In addition to H7 subtype, previous studies also reveal the importance of the residue at position 186 for the receptor binding in other HA subtypes (Liu *et al.*, 2009; Lu *et al.*, 2013a). In avian H2, N186 makes hydrogen bonds with the Gal-2 of the receptor analog through a water molecule, acquiring effective human receptor-binding capacity (Liu *et al.*, 2009). In the H13 subtype, V186 is important for its exclusive avian receptor-binding capacity, and an artificial V186N substitution reduces the binding to the avian receptor analog while increasing the binding to the human receptor analog (Lu *et al.*, 2013a). In the revision course of this manuscript, Tzarum *et al.* (2015) reported the receptor-binding properties of human H6N1 HA (hH6), showing this hH6 still maintains avian receptor-binding preference, which are contradictory to our results. The discrepancy could be potentially explained by different synthetic glycans and other experimental variables. In our case, we performed additional analyses and also did mutagenesis work to confirm the key amino acid substitutions responsible for the receptor-binding change.

Previously, before the appearance of the P186L substitution, the H6N1 viruses persistently circulating in poultry in Taiwan have acquired E190V and G228S substitutions (Wei *et al.*, 2013), which are also helpful for human receptor binding. Currently, the affinity for the human receptor is yet low for most of the H6 subtype viruses, and high affinity for the avian receptor has been maintained, which may hamper the efficient infection and transmission in humans. Moreover, it should be aware that, during the viral entry of the host tissue, the receptor-binding HA is not acting in isolation but in a direct balance with the receptor-cleaving NA (Wagner *et al.*, 2000). Besides receptor binding of HA, HA-NA balance should also be taken into consideration when we evaluate the epidemic or pandemic potential of avian influenza viruses.

Otherwise, the Taiwan hH6N1 virus has not acquired the mammalian-adapted E627K substitution in its PB2, which is also important for efficient infection and transmission in humans (Manz *et al.*, 2013; Wei *et al.*, 2013). However, if the H6N1 virus gains its internal genes from H9N2 (as did the human-infecting H7N9), the E627K mutation may occur and the ability to infect humans might also increase. Therefore, extensive surveillance is crucial to pre-warn against and control potential H6N1 human infections.

Materials and Methods

Solid-phase binding assay

The experiments were performed in approved biosafety level 3 laboratories. The chicken- and human-derived H6N1 viruses were generated by plasmid-based reverse genetics technology (Sun *et al.*, 2011)

to avoid any impurities of the initial isolated viruses (PR8 virus was used as a backbone for the six internal genes, the H6 and N1 genes were derived from A/duck/Taiwan/0526/72, A/chicken/Taiwan/A2837/2013, and A/Taiwan/2/2013, respectively). The rescued viruses were named rDuck-H6N1, rChicken-H6N1, and rHuman-H6N1, respectively, to distinguish them from the natural isolates. All rescued viruses were sequenced to exclude any unwanted mutations. Virus stocks were propagated in specific pathogen-free chicken eggs. Virus concentrations were determined using hemagglutination assays with 1% (v/v) chicken red blood cells. Receptor-binding specificity was analyzed by a solid-phase direct binding assays as described previously (Watanabe *et al*, 2011). Briefly, serial dilutions (0.078125, 0.15625, 0.3125, 0.625, 1.25, 2.5, and 5 µg/ml) of the biotinylated glycans 3'SLNLN and 6'SLNLN were prepared in PBS, and 100 µl was added to the wells of 96-well microtiter plates (Polystyrene Universal-Bind Microplate; Corning)

and allowed to attach overnight at 4°C. The plates were then irradiated with 254 nm ultraviolet light for 2 min. After removal of the glycopolymer solution, the plates were blocked with 0.1 ml PBS containing 2% bovine serum albumin (BSA) at room temperature for 1 h. After washing with ice-cold PBS containing 0.1% Tween-20 (PBST), the plates were incubated in a solution containing influenza virus (64 HA units in PBST) at 4°C for 12 h. After washing with PBST, chicken antisera against the A/duck/Taiwan/0526/72 (Duck-H6N1), A/chicken/Taiwan/A2837/2013 (Chicken-H6N1), A/Taiwan/2/2013 (Human-H6N1), A/California/04/2009 (CA04-H1N1), and A/Anhui/01/2005 (AH05-H5N1) viruses was added to each well, and the plates were incubated at 4°C for 2 h. The wells were then washed with ice-cold PBST and incubated with HRP-linked goat anti-chicken antibody (Sigma-Aldrich, www.sigmaaldrich.com) for 2 h at 4°C. After washing with ice-cold PBST, the plates were incubated with O-phenylenediamine in PBS containing 0.01% H₂O₂ for 10 min at

Table 2. Statistics for crystallographic data collection and structure refinement for Chicken H6.

| | Chicken H6 | Chicken H6-2,3 | Chicken H6-2,6 |
|---|------------------------|------------------------|------------------------|
| Data collection | | | |
| Space group | P21 | P3 | P3 |
| Cell dimensions | | | |
| <i>a</i> , <i>b</i> , <i>c</i> (Å) | 67.61, 106.26, 125.28 | 96.77, 96.77, 132.51 | 97.06, 97.06, 131.68 |
| α , β , γ (°) | 90, 102.75, 90 | 90, 90, 120 | 90, 90, 120 |
| Resolution (Å) | 50.00–2.60 (2.69–2.60) | 50.00–3.00 (3.11–3.00) | 50.00–3.10 (3.21–3.10) |
| <i>R</i> _{merge} | 0.115 (0.872) | 0.100 (0.834) | 0.118 (0.812) |
| <i>I</i> / σ <i>I</i> | 12.5 (1.8) | 13.9 (2.2) | 8.5 (1.5) |
| Completeness (%) | 99.5 (99.9) | 99.0 (100.0) | 92.6 (93.9) |
| Redundancy | 3.9 (3.9) | 4.2 (4.2) | 3.5 (3.4) |
| Refinement | | | |
| Resolution (Å) | 41.37–2.60 | 45.45–3.00 | 45.54–3.10 |
| Number of reflections | 53,268 | 27,681 | 23,294 |
| <i>R</i> _{work} / <i>R</i> _{free} | 0.2200/0.2714 | 0.1986/0.2260 | 0.2095/0.2542 |
| Number of atoms | | | |
| Protein | 11,626 | 7,880 | 7,880 |
| Water | 69 | 0 | 0 |
| Ligand | 0 | 92 | 64 |
| B-factors | | | |
| Protein | 60.9 | 93.7 | 112.3 |
| Water | 76.9 | | |
| Ligand | | 107.7 | 117.7 |
| R.m.s. deviations | | | |
| Bond lengths (Å) | 0.008 | 0.007 | 0.005 |
| Bond angles (°) | 1.489 | 1.001 | 0.966 |
| Ramachandran plot (%) | | | |
| Most favoured regions | 86.1 | 85.5 | 83.6 |
| Additional allowed regions | 13.1 | 13.8 | 15.2 |
| Generously allowed regions | 0.8 | 0.7 | 1.2 |
| Disallowed regions | 0.1 | 0 | 0 |

Values in parentheses are for the highest resolution shell.

room temperature. The reaction was stopped with 0.05 ml 1 M H₂SO₄, and the absorbance was determined at 450 nm.

Gene cloning, protein expression, and purification

The sequences encoding the ectodomain of the HAs from A/duck/Taiwan/0526/72, A/Taiwan/2/2013(hH6), A/Chicken/Taiwan/A2837/2013(cH6), and its mutants were cloned into the baculovirus transfer vector pFastBac1 (Invitrogen) as previously described (Stevens *et al*, 2004; Zhang *et al*, 2010; Shi *et al*, 2013b), in-frame with an N-terminal gp67 signal peptide for secretion, a C-terminal thrombin cleavage site, a trimerization foldon sequence, and a His₆ tag at the extreme C-terminus for purification. Transfection and virus amplification were performed according to the Bac-to-Bac baculovirus expression system manual (Invitrogen).

HA proteins were produced by infecting suspension cultures of Hi5™ cells (Invitrogen) for 2 days. Soluble HA was recovered from

cell supernatants by metal affinity chromatography using a 5-ml HisTrap HP column (GE Healthcare) and then purified by ion-exchange chromatography (IEX) using a Mono-Q4.6/100PE column (GE Healthcare). The purified proteins were subjected to thrombin digestion (BD Biosciences, 3 U/mg HA; overnight at 4°C) to remove the C-terminal trimerization foldon sequence and His₆ tag. For crystallization, the proteins were further purified by gel filtration chromatography using a Superdex®-200 16/60 GL column (GE Healthcare) with a running buffer (pH 8.0) of 20 mM Tris-HCl and 50 mM NaCl. The collected protein fractions were concentrated to 8 mg/ml.

Crystallization, data collection, and structure determination

hH6 and cH6 were both crystallized via the sitting-drop vapor diffusion method at 18°C. The Human-H6N1 crystals grew in a reservoir solution of 0.2 M ammonium acetate, 0.1 M sodium

Table 3. Statistics for crystallographic data collection and structure refinement for Human H6.

| | Human H6 | Human H6-2,3 | Human H6-2,6 |
|---|------------------------|------------------------|------------------------|
| Data collection | | | |
| Space group | P63 | P63 | P63 |
| Cell dimensions | | | |
| <i>a</i> , <i>b</i> , <i>c</i> (Å) | 113.90, 113.90, 163.84 | 114.19, 114.19, 164.96 | 114.39, 114.39, 166.05 |
| α, β, γ (°) | 90, 90, 120 | 90, 90, 120 | 90, 90, 120 |
| Resolution (Å) | 50.00–2.60 (2.69–2.60) | 50.00–2.60 (2.69–2.60) | 50.00–2.60 (2.69–2.60) |
| <i>R</i> _{merge} | 0.109 (0.554) | 0.126 (0.494) | 0.137 (0.846) |
| <i>I</i> / <i>σI</i> | 19.4 (5.3) | 22.0 (6.8) | 21.2 (3.8) |
| Completeness (%) | 99.9 (99.9) | 99.9 (100.0) | 99.9 (99.9) |
| Redundancy | 7.3 (7.6) | 13.1 (13.2) | 12.2 (12.6) |
| Refinement | | | |
| Resolution (Å) | 47.23–2.60 | 46.95–2.60 | 39.77–2.60 |
| Number of reflections | 36,901 | 37,568 | 37,317 |
| <i>R</i> _{work} / <i>R</i> _{free} | 0.1914/0.2247 | 0.1821/0.2082 | 0.1924/0.2265 |
| Number of atoms | | | |
| Protein | 3,938 | 4,016 | 3,938 |
| Water | 188 | 136 | 91 |
| Ligand | 0 | 57 | 32 |
| B-factors | | | |
| Protein | 47.7 | 45.8 | 59.3 |
| Water | 48.9 | 44.5 | 52.8 |
| Ligand | | 100.7 | 120.4 |
| R.m.s. deviations | | | |
| Bond lengths (Å) | 0.007 | 0.006 | 0.008 |
| Bond angles (°) | 1.047 | 1.037 | 1.111 |
| Ramachandran plot (%) | | | |
| Most favoured regions | 87.8 | 88.3 | 87.8 |
| Additional allowed regions | 11.2 | 10.8 | 11.2 |
| Generously allowed regions | 1 | 0.9 | 1 |
| Disallowed regions | 0 | 0 | 0 |

Values in parentheses are for the highest resolution shell.

acetate pH 4.0, and 15% w/v PEG 4000. The Avian-H6N1 crystals grew in a reservoir solution of 0.2 M sodium thiocyanate and 20% w/v polyethylene glycol 3350. For receptor analog complexes, crystals were soaked in a reservoir solution containing 10 mM LSTA ($\text{NeuAc}\alpha2\text{-}3\text{Gal}\beta1\text{-}4\text{GlcNAc}\beta1\text{-}3\text{Gal}\beta1\text{-}4\text{Glc}$) or LSTc ($\text{NeuAc}\alpha2\text{-}6\text{Gal}\beta1\text{-}4\text{GlcNAc}\beta1\text{-}3\text{Gal}\beta1\text{-}4\text{Glc}$) for 4 h. All crystals were flash-cooled in liquid nitrogen after a brief soaking in reservoir solution with the addition of 17% (v/v) glycerol. The X-ray diffraction data were collected at the Shanghai Synchrotron Radiation Facility (SSRF) beamline 17U. All data were processed with HKL2000 software.

The hH6 and cH6 structures were solved by molecular replacement using Phaser from the CCP4 program suite, with the structure of the H2 HA (PDB code: 2WRD) as a model. The HA receptor analog complexes were subsequently determined using the refined HA structure as the input model. The receptor analogs were manually built using COOT based on the simulated annealing omit Fo–Fc maps and were further refined by PHENIX. Final statistics for data collection and structure refinement are represented in Tables 2 and 3. The stereochemical quality of the final model was assessed with the program PROCHECK.

SPR experiments

The affinity and binding kinetics of Duck-H6N1 HA, Human-H6N1 HA, Chicken-H6N1 HA, and its mutants for receptor analogs were both analyzed at 25°C on a BIACore® 3000 machine with streptavidin chips (SA chips, GE Healthcare). PBST was used as the kinetics analysis buffer. Two biotinylated receptor analogs, the α -2,6 glycan (6'SLNLN: NeuAc $\alpha2\text{-}6\text{Gal}\beta1\text{-}4\text{GlcNAc}\beta1\text{-}3\text{Gal}\beta1\text{-}4\text{GlcNAc}\beta1\text{-}6\text{NH-LC-LC-Biotin}$), and the α -2,3 glycan (3'SLNLN: NeuAc $\alpha2\text{-}3\text{Gal}\beta1\text{-}4\text{GlcNAc}\beta1\text{-}3\text{Gal}\beta1\text{-}4\text{GlcNAc}\beta1\text{-}6\text{NH-LC-LC-Biotin}$) were kindly provided by the Consortium for Functional Glycomics (Scripps Research Institute, Department of Molecular Biology, La Jolla, CA). Approximately 400 response units of biotinylated glycans were immobilized on the chip, and a blank channel was used as the negative control. Thrombin-digested HAs were purified by gel filtration using PBST buffer as running buffer and serially diluted to concentrations ranging from 12.5 to 800 μM . The HA protein preparations were then flowed through the chip, and the response units were measured. The sensor surface was regenerated with 10 mM NaOH at the end of each cycle. Sensorgrams were locally fitted with BIACore® 3000 analysis software (BIAsimulation® version 4.1) using a 1:1 Langmuir binding mode and HA monomer as the identity to assume a 1:1 binding. The affinity values of duck- and chicken-H6N1 HAs to receptors were calculated with a Kinetics simultaneous k_a/k_d affinity model, and the affinity values of human-H6N1 HA and chicken-H6N1 HA mutants to receptor were calculated with a steady state affinity model.

Acknowledgements

This work was supported, in part, by the China Ministry of Science and Technology National 973 Project (Grant No. 2011CB504703), the National Natural Science Foundation of China (NSFC, Grant No. 31402196), Strategic Priority Research Program of the Chinese Academy of Sciences (XDB08020100), Intramural Special Grant for Influenza Virus Research from the Chinese Academy of Sciences (KJZD-EW-L09), and the China National

Grand S&T Special Project (Grant No. 2014ZX10004002). G.F.G. is a leading principal investigator of the NSFC Innovative Research Group (Grant No. 81321063). Y.S. is supported by the Excellent Young Scientist Program of the Chinese Academy of Sciences.

Author contributions

GFG designed and coordinated the study. FW, WZ, and MinW conducted the experiments. JQ collected the datasets and solved the structures. YS and GFG wrote the manuscript, and BZ, MingW, JL, and JY participated in the manuscript editing and discussion.

Conflict of interest

The authors declare that they have no conflict of interest.

References

- Baum LG, Paulson JC (1991) The N2 neuraminidase of human influenza virus has acquired a substrate specificity complementary to the hemagglutinin receptor specificity. *Virology* 180: 10–15
- Chen H, Yuan H, Gao R, Zhang J, Wang D, Xiong Y, Fan G, Yang F, Li X, Zhou J, Zou S, Yang L, Chen T, Dong L, Bo H, Zhao X, Zhang Y, Lan Y, Bai T, Dong J et al (2014) Clinical and epidemiological characteristics of a fatal case of avian influenza A H10N8 virus infection: a descriptive study. *Lancet* 383: 714–721
- Choi YK, Seo SH, Kim JA, Webby RJ, Webster RG (2005) Avian influenza viruses in Korean live poultry markets and their pathogenic potential. *Virology* 332: 529–537
- Claas EC, Osterhaus AD, van Beek R, De Jong JC, Rimmelzwaan GF, Senne DA, Krauss S, Shortridge KF, Webster RG (1998) Human influenza A H5N1 virus related to a highly pathogenic avian influenza virus. *Lancet* 351: 472–477
- Connor RJ, Kawaoka Y, Webster RG, Paulson JC (1994) Receptor specificity in human, avian, and equine H2 and H3 influenza virus isolates. *Virology* 205: 17–23
- Corrand L, Delverdier M, Lucas MN, Croville G, Facon C, Balloy D, Ducatez M, Guerin JL (2012) A low-pathogenic avian influenza H6N1 outbreak in a turkey flock in France: a comprehensive case report. *Avian Pathol* 41: 569–577
- de Graaf M, Fouchier RA (2014) Role of receptor binding specificity in influenza A virus transmission and pathogenesis. *EMBO J* 33: 1614
- de Wit E, Munster VJ, van Riel D, Beyer WE, Rimmelzwaan GF, Kuiken T, Osterhaus AD, Fouchier RA (2010) Molecular determinants of adaptation of highly pathogenic avian influenza H7N7 viruses to efficient replication in the human host. *J Virol* 84: 1597–1606
- Eisen MB, Sabesan S, Skehel JJ, Wiley DC (1997) Binding of the influenza A virus to cell-surface receptors: structures of five hemagglutinin-sialyloigosaccharide complexes determined by X-ray crystallography. *Virology* 232: 19–31
- Gambaryan AS, Tuzikov AB, Piskarev VE, Yamnikova SS, Lvov DK, Robertson JS, Bovin NV, Matrosovich MN (1997) Specification of receptor-binding phenotypes of influenza virus isolates from different hosts using synthetic sialylglycopolymers: non-egg-adapted human H1 and H3 influenza A and influenza B viruses share a common high binding affinity for 6'-sialyl(N-acetyllactosamine). *Virology* 232: 345–350
- Gamblin SJ, Haire LF, Russell RJ, Stevens DJ, Xiao B, Ha Y, Vasisht N, Steinhauer DA, Daniels RS, Elliot A, Wiley DC, Skehel JJ (2004) The structure and receptor binding properties of the 1918 influenza hemagglutinin. *Science* 303: 1838–1842

- Gamblin SJ, Skehel JJ (2010) Influenza hemagglutinin and neuraminidase membrane glycoproteins. *J Biol Chem* 285: 28403–28409
- Gao R, Cao B, Hu Y, Feng Z, Wang D, Hu W, Chen J, Jie Z, Qiu H, Xu K, Xu X, Lu H, Zhu W, Gao Z, Xiang N, Shen Y, He Z, Gu Y, Zhang Z, Yang Y et al (2013) Human infection with a novel avian-origin influenza A (H7N9) virus. *N Engl J Med* 368: 1888–1897
- Gregg MB, Hinman AR, Craven RB (1978) The Russian flu. Its history and implications for this year's influenza season. *JAMA* 240: 2260–2263
- Guo Y, Li J, Cheng X (1999) [Discovery of men infected by avian influenza A (H9N2) virus]. *Chin J Exp Clin Virol* 13: 105–108
- Ha Y, Stevens DJ, Skehel JJ, Wiley DC (2001) X-ray structures of H5 avian and H9 swine influenza virus hemagglutinins bound to avian and human receptor analogs. *Proc Natl Acad Sci USA* 98: 11181–11186
- Herfst S, Schrauwen EJ, Linster M, Chutinimitkul S, de Wit E, Munster VJ, Sorrell EM, Bestebroer TM, Burke DF, Smith DJ, Rimmelzwaan GF, Osterhaus AD, Fouchier RA (2012) Airborne transmission of influenza A/H5N1 virus between ferrets. *Science* 336: 1534–1541
- Imai M, Kawaoka Y (2012) The role of receptor binding specificity in interspecies transmission of influenza viruses. *Curr Opin Virol* 2: 160–167
- Imai M, Watanabe T, Hatta M, Das SC, Ozawa M, Shinya K, Zhong G, Hanson A, Katsura H, Watanabe S, Li C, Kawakami E, Yamada S, Kiso M, Suzuki Y, Maher EA, Neumann G, Kawaoka Y (2012) Experimental adaptation of an influenza H5 HA confers respiratory droplet transmission to a reassortant H5 HA/H1N1 virus in ferrets. *Nature* 486: 420–428
- Jagger BW, Wise HM, Kash JC, Walters KA, Wills NM, Xiao YL, Dunfee RL, Schwartzman LM, Ozinsky A, Bell GL, Dalton RM, Lo A, Efstratiou S, Atkins JF, Firth AE, Taubenberger JK, Digard P (2012) An overlapping protein-coding region in influenza A virus segment 3 modulates the host response. *Science* 337: 199–204
- Koopmans M, Wilbrink B, Conyn M, Natrop G, van der Nat H, Vennema H, Meijer A, van Steenbergen J, Fouchier R, Osterhaus A, Bosman A (2004) Transmission of H7N7 avian influenza A virus to human beings during a large outbreak in commercial poultry farms in the Netherlands. *Lancet* 363: 587–593
- Lee MS, Chang PC, Shien JH, Cheng MC, Chen CL, Shieh HK (2006) Genetic and pathogenic characterization of H6N1 avian influenza viruses isolated in Taiwan between 1972 and 2005. *Avian Dis* 50: 561–571
- Li Q, Sun X, Li Z, Liu Y, Vavricka CJ, Qi J, Gao GF (2012) Structural and functional characterization of neuraminidase-like molecule N10 derived from bat influenza A virus. *Proc Natl Acad Sci USA* 109: 18897–18902
- Lin YP, Xiong X, Wharton SA, Martin SR, Coombs PJ, Vachieri SG, Christodoulou E, Walker PA, Liu J, Skehel JJ, Gamblin SJ, Hay AJ, Daniels RS, McCauley JW (2012) Evolution of the receptor binding properties of the influenza A(H3N2) hemagglutinin. *Proc Natl Acad Sci USA* 109: 21474–21479
- Liu C, Eichelberger MC, Compans RW, Air GM (1995) Influenza type A virus neuraminidase does not play a role in viral entry, replication, assembly, or budding. *J Virol* 69: 1099–1106
- Liu J, Stevens DJ, Haire LF, Walker PA, Coombs PJ, Russell RJ, Gamblin SJ, Skehel JJ (2009) Structures of receptor complexes formed by hemagglutinins from the Asian Influenza pandemic of 1957. *Proc Natl Acad Sci USA* 106: 17175–17180
- Lu X, Shi Y, Gao F, Xiao H, Wang M, Qi J, Gao GF (2012) Insights into avian influenza virus pathogenicity: the hemagglutinin precursor HA0 of subtype H16 has an alpha-helix structure in its cleavage site with inefficient HA1/HA2 cleavage. *J Virol* 86: 12861–12870
- Lu X, Qi J, Shi Y, Wang M, Smith DF, Heimburg-Molinaro J, Zhang Y, Paulson JC, Xiao H, Gao GF (2013a) Structure and receptor binding specificity of hemagglutinin H13 from avian influenza A virus H13N6. *J Virol* 87: 9077–9085
- Lu X, Shi Y, Zhang W, Zhang Y, Qi J, Gao GF (2013b) Structure and receptor-binding properties of an airborne transmissible avian influenza A virus hemagglutinin H5 (VN1203mut). *Protein Cell* 4: 502–511
- Manz B, Schwemmle M, Brunotte L (2013) Adaptation of avian influenza A virus polymerase in mammals to overcome the host species barrier. *J Virol* 87: 7200–7209
- Muzyska D, Pantin-Jackwood M, Spackman E, Stegniy B, Rula O, Shutchenko P (2012) Avian influenza virus wild bird surveillance in the Azov and Black Sea regions of Ukraine (2010–2011). *Avian Dis* 56: 1010–1016
- Ohuchi M, Ohuchi R, Feldmann A, Klunk HD (1997) Regulation of receptor binding affinity of influenza virus hemagglutinin by its carbohydrate moiety. *J Virol* 71: 8377–8384
- Palese P, Tobita K, Ueda M, Compans RW (1974) Characterization of temperature sensitive influenza virus mutants defective in neuraminidase. *Virology* 61: 397–410
- Sauter NK, Bednarski MD, Wurzburg BA, Hanson JE, Whitesides GM, Skehel JJ, Wiley DC (1989) Hemagglutinins from two influenza virus variants bind to sialic acid derivatives with millimolar dissociation constants: a 500-MHz proton nuclear magnetic resonance study. *Biochemistry* 28: 8388–8396
- Shenderovich SF, Molibog EV, Iakhno MA, Zakstelskaia L, Zhdanov VM (1979) [Antigenic and biological characteristics of the A (H1N1) strains that caused the 1977–1978 epidemic]. *Vopr Virusol* 5: 480–486
- Shi W, Shi Y, Wu Y, Liu D, Gao GF (2013a) Origin and molecular characterization of the human-infecting H6N1 influenza virus in Taiwan. *Protein Cell* 4: 846–853
- Shi Y, Zhang W, Wang F, Qi J, Wu Y, Song H, Gao F, Bi Y, Zhang Y, Fan Z, Qin C, Sun H, Liu J, Haywood J, Liu W, Gong W, Wang D, Shu Y, Wang Y, Yan J et al (2013b) Structures and receptor binding of hemagglutinins from human-infecting H7N9 influenza viruses. *Science* 342: 243–247
- Shi Y, Wu Y, Zhang W, Qi J, Gao GF (2014) Enabling the 'host jump': structural determinants of receptor-binding specificity in influenza A viruses. *Nat Rev Microbiol* 12: 822–831
- Siembieda JL, Johnson CK, Cardona C, Anchell N, Dao N, Reisen W, Boyce W (2010) Influenza A viruses in wild birds of the Pacific flyway, 2005–2008. *Vector Borne Zoonotic Dis* 10: 793–800
- Stevens J, Corper AL, Basler CF, Taubenberger JK, Palese P, Wilson IA (2004) Structure of the uncleaved human H1 hemagglutinin from the extinct 1918 influenza virus. *Science* 303: 1866–1870
- Sun Y, Qin K, Wang J, Pu J, Tang Q, Hu Y, Bi Y, Zhao X, Yang H, Shu Y, Liu J (2011) High genetic compatibility and increased pathogenicity of reassortants derived from avian H9N2 and pandemic H1N1/2009 influenza viruses. *Proc Natl Acad Sci USA* 108: 4164–4169
- Sun X, Shi Y, Lu X, He J, Gao F, Yan J, Qi J, Gao GF (2013) Bat-derived influenza hemagglutinin H17 does not bind canonical avian or human receptors and most likely uses a unique entry mechanism. *Cell Rep* 3: 769–778
- Taubenberger JK, Morens DM (2008) The pathology of influenza virus infections. *Annu Rev Pathol* 3: 499–522
- Taubenberger JK, Kash JC (2010) Influenza virus evolution, host adaptation, and pandemic formation. *Cell Host Microbe* 7: 440–451
- Tong S, Li Y, Rivaillet P, Conrardy C, Castillo DA, Chen LM, Recuenco S, Ellison JA, Davis CT, York IA, Turmelle AS, Moran D, Rogers S, Shi M, Tao Y, Weil MR, Tang K, Rowe LA, Sammons S, Xu X et al (2012) A distinct lineage of influenza A virus from bats. *Proc Natl Acad Sci USA* 109: 4269–4274

- Tong S, Zhu X, Li Y, Shi M, Zhang J, Bourgeois M, Yang H, Chen X, Recuenco S, Gomez J, Chen LM, Johnson A, Tao Y, Dreyfus C, Yu W, McBride R, Carney PJ, Gilbert AT, Chang J, Guo Z et al (2013) New world bats harbor diverse influenza A viruses. *PLoS Pathog* 9: e1003657
- Tzarum N, de Vries RP, Zhu X, Yu W, McBride R, Paulson JC, Wilson IA (2015) Structure and Receptor Binding of the Hemagglutinin from a Human H6N1 Influenza Virus. *Cell Host Microbe* 17: 369–376
- Vachieri SG, Xiong X, Collins PJ, Walker PA, Martin SR, Haire LF, Zhang Y, McCauley JW, Gamblin SJ, Skehel JJ (2014) Receptor binding by H10 influenza viruses. *Nature* 511: 475–477
- Wagner R, Wolff T, Herwig A, Pleschka S, Klenk HD (2000) Interdependence of hemagglutinin glycosylation and neuraminidase as regulators of influenza virus growth: a study by reverse genetics. *J Virol* 74: 6316–6323
- Wang G, Deng G, Shi J, Luo W, Zhang G, Zhang Q, Liu L, Jiang Y, Li C, Sriwilaijaroen N, Hiramatsu H, Suzuki Y, Kawaoka Y, Chen H (2014) H6 influenza viruses pose a potential threat to human health. *J Virol* 88: 3953–3964
- Watanabe Y, Ibrahim MS, Ellakany HF, Kawashita N, Mizuike R, Hiramatsu H, Sriwilaijaroen N, Takagi T, Suzuki Y, Ikuta K (2011) Acquisition of human-type receptor binding specificity by new H5N1 influenza virus sublineages during their emergence in birds in Egypt. *PLoS Pathog* 7: e1002068
- Wei SH, Yang JR, Wu HS, Chang MC, Lin JS, Lin CY, Liu YL, Lo YC, Yang CH, Chuang JH, Lin MC, Chung WC, Liao CH, Lee MS, Huang WT, Chen PJ, Liu MT, Chang FY (2013) Human infection with avian influenza A H6N1 virus: an epidemiological analysis. *Lancet Respir Med* 1: 771–778
- Wu Y, Wu Y, Tefsen B, Shi Y, Gao GF (2014) Bat-derived influenza-like viruses H17N10 and H18N11. *Trends Microbiol* 22: 183–191
- Xiong X, Coombs PJ, Martin SR, Liu J, Xiao H, McCauley JW, Locher K, Walker PA, Collins PJ, Kawaoka Y, Skehel JJ, Gamblin SJ (2013a) Receptor binding by a ferret-transmissible H5 avian influenza virus. *Nature* 497: 392–396
- Xiong X, Martin SR, Haire LF, Wharton SA, Daniels RS, Bennett MS, McCauley JW, Collins PJ, Walker PA, Skehel JJ, Gamblin SJ (2013b) Receptor binding by an H7N9 influenza virus from humans. *Nature* 499: 496–499
- Xu R, de Vries RP, Zhu X, Nycholat CM, McBride R, Yu W, Paulson JC, Wilson IA (2013) Preferential recognition of avian-like receptors in human influenza A H7N9 viruses. *Science* 342: 1230–1235
- Xu R, McBride R, Nycholat CM, Paulson JC, Wilson IA (2012) Structural characterization of the hemagglutinin receptor specificity from the 2009 H1N1 influenza pandemic. *J Virol* 86: 982–990
- Yang H, Carney PJ, Chang JC, Villanueva JM, Stevens J (2013) Structural analysis of the hemagglutinin from the recent 2013 H7N9 influenza virus. *J Virol* 87: 12433–12446
- Yuan J, Zhang L, Kan X, Jiang L, Yang J, Guo Z, Ren Q (2013) Origin and molecular characteristics of a novel 2013 avian influenza A(H6N1) virus causing human infection in Taiwan. *Clin Infect Dis* 57: 1367–1368
- Yuen KY, Chan PK, Peiris M, Tsang DN, Que TL, Shortridge KF, Cheung PT, To WK, Ho ET, Sung R, Cheng AF (1998) Clinical features and rapid viral diagnosis of human disease associated with avian influenza A H5N1 virus. *Lancet* 351: 467–471
- Zhang W, Qi J, Shi Y, Li Q, Gao F, Sun Y, Lu X, Lu Q, Vavricka CJ, Liu D, Yan J, Gao GF (2010) Crystal structure of the swine-origin A (H1N1)-2009 influenza A virus hemagglutinin (HA) reveals similar antigenicity to that of the 1918 pandemic virus. *Protein Cell* 1: 459–467
- Zhang W, Shi Y, Lu X, Shu Y, Qi J, Gao GF (2013a) An airborne transmissible avian influenza H5 hemagglutinin seen at the atomic level. *Science* 340: 1463–1467
- Zhang W, Shi Y, Qi J, Gao F, Li Q, Fan Z, Yan J, Gao GF (2013b) Molecular basis of the receptor binding specificity switch of the hemagglutinins from both the 1918 and 2009 pandemic influenza A viruses by a D225G substitution. *J Virol* 87: 5949–5958
- Zhu X, Yang H, Guo Z, Yu W, Carney PJ, Li Y, Chen LM, Paulson JC, Donis RO, Tong S, Stevens J, Wilson IA (2012) Crystal structures of two subtype N10 neuraminidase-like proteins from bat influenza A viruses reveal a diverged putative active site. *Proc Natl Acad Sci USA* 109: 18903–18908
- Zhu X, Yu W, McBride R, Li Y, Chen LM, Donis RO, Tong S, Paulson JC, Wilson IA (2013) Hemagglutinin homologue from H17N10 bat influenza virus exhibits divergent receptor-binding and pH-dependent fusion activities. *Proc Natl Acad Sci USA* 110: 1458–1463